PHYSICAL REVIEW C **77**, 011302(R) (2008)

Isospin effects on the evaporation residue spin distribution

W. Ye, H. W. Yang, and F. Wu
Department of Physics, Southeast University, Nanjing 210096, People's Republic of China
(Received 25 October 2007; revised manuscript received 10 December 2007; published 29 January 2008)

Based on a Langevin equation coupled with a statistical decay model, we have studied the evaporation residue spin distribution of the nuclei ^{194}Pb, ^{200}Pb, ^{200}Pb, and ^{200}Os, and extracted a presaddle nuclear dissipation strength of 5×10^{21} s^{-1} by comparing our results with the measured spin distribution of ^{200}Pb produced in the ^{16}O + ^{184}W reaction. We find that with increasing isospin of the system, the sensitivity of the spin distribution to nuclear dissipation decreases substantially. Moreover, for ^{200}Os, this spin distribution is no longer sensitive to the nuclear dissipation. These results suggest that on the experimental side, to accurately obtain the information of presaddle dissipation strength by measuring the evaporation residue spin distribution, it is best to populate those systems with low isospin.

DOI: 10.1103/PhysRevC.77.011302 PACS number(s): 25.70.Jj, 24.10.−i, 24.75.+i, 27.80.+w

The nature and magnitude of nuclear dissipation is one of the most interesting and challenging problems in nuclear physics. In particular, presaddle nuclear dissipation strength is the focus of current experimental [1–5] and theoretical [6–8] research on the fission of highly excited nuclei. Because prescission light particles [9] and giant dipole resonance (GDR) γ rays [10] arise from the contribution of both presaddle and saddle-to-scission emission, it is very difficult to determine the presaddle dissipation strength by merely using the particle multiplicity. Under this circumstance, it is necessary to search for new observables that only depend on the presaddle dissipation effects. Besides the evaporation residue cross section [11,12] and the width of the fission-fragment charge distribution [1,4], the spin distribution of the evaporation residue cross section, namely, the angular momentum distribution leading to evaporation residues, may be a new and an extremely sensitive probe of the presaddle dissipation strength, as suggested in Ref. [13].

To extract a precise value of dissipation strength by comparing theoretical predictions with experiment, a Langevin model is certainly preferable to a statistical model. This is because the Langevin model considers the time evolution of the fission decay width and contains a number of dynamical features in the decay of the hot compound nuclei, e.g., the angular momentum dependence of presaddle and saddle-to-scission time, etc. These advantages are not considered in a simple statistical model analysis. In addition, the Langevin model has been employed [14–18] to successfully reproduce a great deal of experimental data on prescission particle multiplicity, evaporation evaporation cross sections, and kinetic distributions of fission fragments over a wide range of excitation energy, angular momentum, and fissility.

The present work is devoted to the study of the favorable experimental condition through which presaddle dissipation effects can be better revealed with evaporation residue spin distributions. For this aim, we use the Langevin model to reproduce the measured evaporation residue spin distribution of ^{200}Pb populated in the ^{16}O + ^{184}W reaction that will provide a stringent test for the widely accepted fission model and also shed new light on the magnitude of presaddle dissipation strength. Besides, it has been reported that isospin has a strong effect on light charged particles [19] and GDR γ-ray emission [7] as a probe of nuclear dissipation. In this context, to better instruct experimental exploration, we will survey the isospin effect on the evaporation residue spin distribution as a probe of nuclear dissipation.

Here we introduce briefly a combined dynamical and statistical model (CDSM) [14,20]. For a review of the model, we refer the reader to Ref. [14]. The dynamical part of the CDSM is described by the Langevin equation which is expressed by the free energy F. In the Fermi gas model, F is related to the level density parameter $a(q)$ by

$$F(q, T) = V(q) - a(q)T^2, \tag{1}$$

where $V(q)$ is the fission potential and T is the nuclear temperature. The level density parameter $a(q)$ is taken from the work of Ignatyuk *et al.* [21].

The one-dimensional overdamped Langevin equation reads

$$\frac{dq}{dt} = -\frac{1}{M\beta(q)}\frac{\partial F(q, T)_T}{\partial q} + \sqrt{D(q)}\Gamma(t), \tag{2}$$

where q is the dimensionless fission coordinate and defined as half the distance between the centers of mass of the future fission fragments divided by the radius of the compound nucleus. $\beta(q)$ is the dissipation strength. The fluctuation strength coefficient $D(q)$ can be expressed according to the fluctuation-dissipation theorem as

$$D(q) = \frac{T}{M\beta(q)}, \tag{3}$$

where M is the inertia parameter which drops out of the overdamped equation. $\Gamma(t)$ is a time-dependent stochastic variable with Gaussian distribution. Its average and correlation function are written as

$$\begin{aligned} \langle\Gamma(t)\rangle &= 0, \\ \langle\Gamma(t)\Gamma(t')\rangle &= 2\delta(t - t'). \end{aligned} \tag{4}$$

The potential energy $V(Z, A, L, q)$ is given by the liquid-drop expression [22]

$$V(A, Z, L, q) = a_2\left[1 - k\left(\frac{N-Z}{A}\right)^2\right]A^{2/3}[B_s(q) - 1] + c_3\frac{Z^2}{A^{1/3}}[B_c(q) - 1] + c_r L^2 A^{-5/3} B_r(q), \quad (5)$$

Here we have dropped terms that do not depend on the deformation coordinate q. The parameters a_2, c_3, k, and c_r in Eq. (5) are taken from Ref. [23]. $B_s(q)$, $B_c(q)$, and $B_r(q)$ are the surface, Coulomb, and rotational energy terms, respectively. The present model uses the well-known "funny hills" parameters $\{c, h, \alpha\}$ [24] to describe the surface of the nucleus. Since only symmetrical fission is considered, the parameter describing the asymmetry of the shape $\alpha = 0$ [14,25]. The dimensionless fission coordinate q is obtained by the relation $q(c, h) = (3c/8)(1 + \frac{2}{15}[2h + (c-1)/2]c^3)$ [14,26], where c and h correspond to the elongation and neck degrees of freedom of the nucleus, respectively. B_r is proportional to the inverse of the rigid body moment of inertia [27]. For more details about how to calculate the shape dependence of B_s, B_c, and B_r, see Refs. [14,27].

When the dynamical description reaches a quasistationary regime, the CDSM switches over to a statistical model; that is, the decay of the compound system is described by the statistical part of the CDSM. In the CDSM, the light-particle evaporation is coupled to the fission mode by a Monte Carlo procedure allowing for the discrete emission of light particles. The widths for light particles (n, p, α) and GDR γ decay are given by the parametrization of Blann [28] and Lynn [29], respectively.

The spin distribution of the evaporation residue cross section only depends on the dissipation strength inside the barrier. Accordingly, β is chosen here as (3, 5, 7, 10, and 20) $\times$ 10^{21} s^{-1} throughout the fission process. To accumulate sufficient statistics, 5×10^7 Langevin trajectories are simulated. For each trajectory simulating the fission motion, an angular momentum $L = \hbar\ell$ is sampled from the spin distribution of the compound nucleus [14]. The differential

$$\frac{d\sigma(\ell)}{d\ell} = \frac{2\pi}{k^2}\frac{2\ell+1}{1 + \exp[(\ell - \ell_c)/\delta\ell]} \quad (6)$$

describes the fusion process. The final results are weighted over all relevant waves; i.e., the spin distribution is used as the angular momentum weight function. The parameters ℓ_c and $\delta\ell$ are, respectively, the critical angular momentum for fusion and diffuseness. It is found that these parameters for different systems follow an approximate scaling [14], which is in accordance with the surface friction model [14] that describes the fusion cross section very well [30]. Namely,

$$\ell_c = \sqrt{A_p A_T / A_{\rm CN}}\left(A_P^{1/3} + A_T^{1/3}\right) \times (0.33 + 0.205\sqrt{E_{\rm c.m.} - V_c}), \quad (7)$$

when $0 < E_{\rm c.m.} - V_c < 120$ MeV; when $E_{\rm c.m.} - V_c > 120$ MeV, the term in the last bracket is put equal to 2.5. In Eq. (7), A_T and A_P represent the mass of target and projectile, respectively; and $A_{\rm CN}$ is the mass of compound nucleus. For the barrier V_c, an ansatz is used; i.e., $V_c = \frac{5}{3}c_3\frac{A_P A_T}{A_P^{1/3} + A_T^{1/3} + 1.6}$ with $c_3 = 0.7053$ MeV. The diffuseness δl scales as

$$\delta l = \begin{cases} [(A_P A_T)^{3/2} \times 10^{-5}][1.5 + 0.02(E_{\rm c.m.} - V_c - 10)] \\ \quad \text{for} \quad E_{\rm c.m.} > V_c + 10, \\ [(A_P A_T)^{3/2} \times 10^{-5}][1.5 - 0.04(E_{\rm c.m.} - V_c - 10)] \\ \quad \text{for} \quad E_{\rm c.m.} < V_c + 10. \end{cases} \quad (8)$$

Many authors [14,18,25,27] have shown that the scaling values of ℓ_c and δl fit not only the fusion cross section but also a host of experimental observables. Therefore, in this study, we use the scaling values of these parameters.

Figure 1 shows the experimental data and theoretical simulations from which three typical features are observed.

(i) At low beam energy [Figs. 1(a) and 1(b)], the data can be described without dissipation, and using different β values has no significant effect on the calculations. This is because although nuclear dissipation delays the fission process, particle evaporation time is rather long at low energies. Consequently, presaddle particles are not influenced strongly by dissipation (see Fig. 2). Figure 2 shows that $N_{\rm gs}$ changes slightly with increasing β at $E_{\rm lab} = 84$ MeV.

(ii) With increasing beam energy [Figs. 1(c)–1(f)], nuclear dissipation shifts the spin distribution toward high ℓ values, the shift itself becoming larger with increasing β. The interpretation for this feature is that dissipation effects on the presaddle neutrons become stronger with increasing beam energy (see Fig. 2). This occurs because high excitation energy shortens particle evaporation time, thereby enabling particle emission to compete more effectively with fission at a high angular momentum, especially at a larger β. A higher particle emission rate prior to the saddle point favors the evaporation residue survival at high spins [31].

(iii) A presaddle dissipation strength of $\beta = 5 \times 10^{21}$ s^{-1} is needed to reproduce the overall trend of the evaporation residue spin distribution data at the six beam energies investigated since the data are underestimated [Figs. 1(c) and 1(d)] or cannot be described at all at large ℓ values [Fig. 1(f)] if nuclear dissipation effects are not taken into account. Figures 1(c) and 1(d) indicate that both $\beta = 3 \times 10^{21}$ and $\beta = 5 \times 10^{21}$ s^{-1} reproduce the data equally well and a larger viscosity coefficient causes the fit to be less good. Moreover, Fig. 1(f) demonstrates that for $E_{\rm lab} = 120$ MeV, the theoretical spin distribution using $\beta = 3 \times 10^{21}$ s^{-1} is lower than the experimental data at large ℓ, whereas using $\beta = 5 \times 10^{21}$ s^{-1} gives a rather satisfactory description for the data at high spins. It is of interest to compare the resulting presaddle dissipation strength with results of other work. The analysis of prescission light particles found the magnitude of presaddle β to be $\sim 6 \times 10^{21}$ [32], $(5–8) \times 10^{21}$ [33], 3×10^{21} [34], $(3–10) \times 10^{21}$ [35], 5×10^{21} [16], and $<3 \times 10^{21}$ [36] s^{-1}. From the study of GDR γ-ray decay and evaporation residue

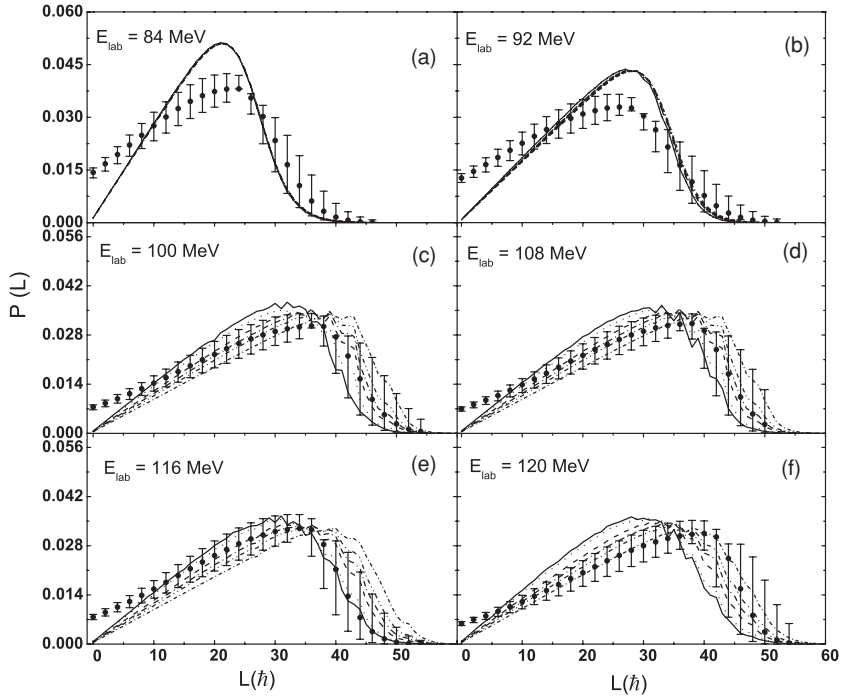

FIG. 1. Evaporation residue spin distributions for the reaction $^{16}O + ^{184}W$ at six beam energies are compared with theoretical calculations for the standard statistical-model case (solid line), $\beta = 3 \times 10^{21}$ (dotted line), $\beta = 5 \times 10^{21}$ (dashed line), $\beta = 7 \times 10^{21}$ (dash dot line), $\beta = 10 \times 10^{21}$ (double-dot dash line), and $\beta = 20 \times 10^{21}$ s^{-1} (short-dash dot line). Experimental data (solid points with error bars) are taken from Ref. [13].

cross sections, the extracted presaddle β is $<8 \times 10^{21}$ [37], $\leqslant 10 \times 10^{21}$ [11], 4×10^{21} [38], and 6×10^{21} [39] s^{-1}. The survey for the mass- and kinetic-energy distributions of fission fragments suggests a presaddle β of 5.5×10^{21} s^{-1} [40–42]. By analyzing fission-fragment charge distributions, presaddle β is found to be 2×10^{21} [4] and $(4.5 \pm 0.5) \times 10^{21}$ [1] s^{-1}. We note that although the specific value of presaddle dissipation strength reported in different literature varies somewhat, on the whole, its magnitude is not strong in comparison to the one-body dissipation prediction, a conclusion that is reached by Fröbrich and Gontchar [14]. In addition, the present β value is very close to those obtained in Refs. [1,16,32,38–42].

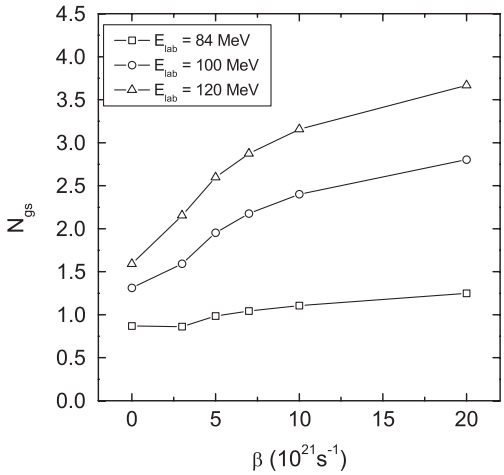

FIG. 2. Comparison of presaddle emitted neutrons (N_{gs}) for the reaction $^{16}O + ^{184}W \longrightarrow ^{200}Pb$ at three beam energies as a function of nuclear dissipation strength (β).

A good fit to the the spin distribution data shows that the Langevin model can yield a realistic quantitative estimate of the evaporation residue population at high angular momenta. On this basis, we investigate the isospin effect on the evaporation residue spin distribution. To this end, four fissioning systems are chosen, namely, ^{194}Pb, ^{200}Pb, ^{206}Pb, and ^{200}Os, whose isospin values (N/Z) are 1.365, 1.439, 1.512, and 1.632, respectively. The dissipation effects on this distribution is to shift the distribution toward the higher ℓ values; therefore, to better reveal this dissipation effect, we define a ratio of the spin distribution evaluated with dissipation to that without

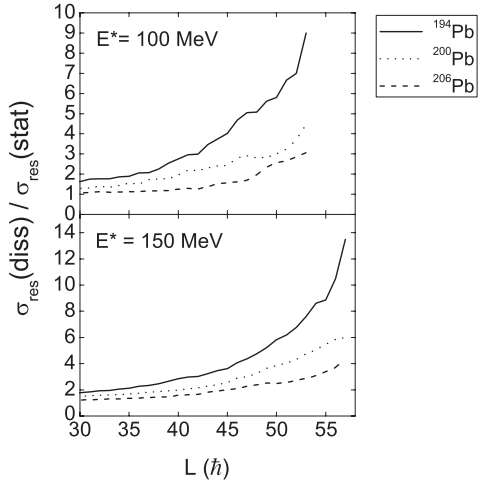

FIG. 3. Ratio of the evaporation residue cross section spin distribution above a given spin evaluated with dissipation (at $\beta = 5 \times 10^{21}$ s^{-1}) to that without dissipation (corresponding to the standard statistical-model case) for three Pb systems at critical angular momentum $\ell_c = 70\hbar$ and two excitation energies.

dissipation above a given spin, that is,

$$R = \frac{\sigma_{\rm res}(\rm diss)}{\sigma_{\rm res}(\rm stat)}. \quad (9)$$

Figure 3 displays calculation results at $\beta = 5 \times 10^{21}$ s^{-1} for the three Pb systems. An increase in R with the isospin of Pb systems is clearly seen from the figure, which shows that the magnitude of dissipation effects has a dependence on the isospin of the system. Take the case of $E^* = 150$ MeV and $\ell_c = 70\hbar$ as an illustration. For ^{206}Pb, the R is 2.48 (3.38) at spin 50 (55)$\hbar$, meaning that because of dissipation, the evaporation residue population at these two spins is increased 1.48 (2.38) times relative to the standard statistical-model prediction. This increase becomes 2.85 (4.48) times for ^{200}Pb, and it rises to 4.83 (7.86) times for ^{194}Pb. At a higher spin of 57$\hbar$, R is 4.36 for ^{206}Pb, which is much smaller than for ^{194}Pb, whose R amounts to 13.5. A physical explanation of the isospin dependence of R stems from the dependence of both the presaddle neutrons and the fission barrier on the isospin of the system. With increasing isospin, the particle separation energy decreases and the fission barrier increases. A high barrier reduces the fission width and protects the system from disintegrating quickly, thus enhancing neutron emission. As a result, for a high-isospin system, the effects on neutron emission coming from the decrement of neutron separation energy and the increment of fission barrier will mask the effects coming from dissipation more strongly than in a low-isospin system. Consequently, the effect of the retardation of the fission process caused by dissipation is clearly manifested as a larger increase in the evaporation residue population for a low-isospin system. In other words, dissipation effects on the spin distribution are amplified at a lower isospin.

To further explore this isospin effect, we plot in Fig. 4 the ratio R for a high-isospin ^{200}Os system. It is evident that R is close to unity regardless of the spin value of evaporation residues, implying an insensitivity of the evaporation residue population to nuclear dissipation. This is different from the situation with ^{200}Pb. Specifically, for ^{200}Pb at $E^* = 150$ MeV and $\ell_c = 50\hbar$, $R = 1.498\,(1.966)$ when spin $\ell = 30\,(40)\hbar$, indicating that dissipation leads to an increase of 49.8% (96.6%) for the evaporation residue population with respect to the statistical model values. In contrast, for ^{200}Os, the corresponding increases at these two spin values are less than 0.1%. A similar picture is observed at another critical angular momentum $\ell_c = 70\hbar$, and it does not change at a smaller excitation energy $E^* = 100$ MeV (left column of Fig. 4). Therefore, the calculation result for ^{200}Os demonstrates that for such a system with even higher isospin, the evaporation residue spin distribution is not a good observable of nuclear dissipation. Based on those conclusions drawn from Figs. 3 and 4, one can see on the experimental side, that populating a low-isospin compound system can significantly enhance the sensitivity of the spin distribution to dissipation effects, in particular at the high angular momentum region. Because these three Pb systems with different isospins can be produced by heavy-ion fusion reactions, current predictions concerning the isospin effect on the evaporation residue spin distribution can be directly compared with the data available in future experiments.

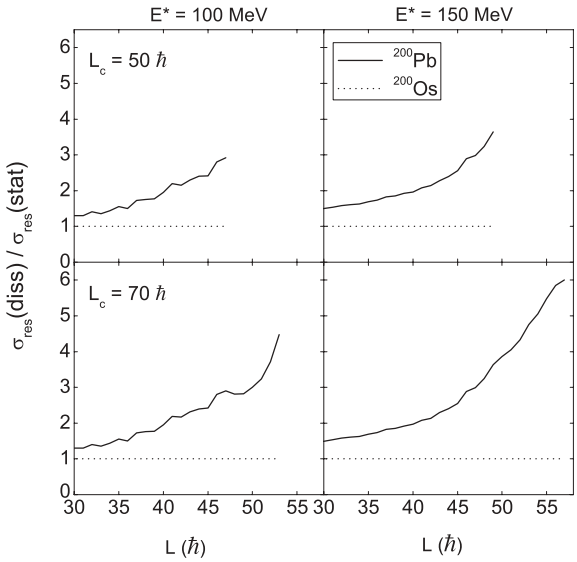

FIG. 4. Ratio of the evaporation residue cross section spin distribution above a given spin evaluated with dissipation (at $\beta = 5 \times 10^{21}$ s^{-1}) to that without dissipation (corresponding to the statistical-model case) for systems ^{200}Pb and ^{200}Os at two excitation energies and two critical angular momenta.

Finally, it should be mentioned that we also performed calculations at other dissipation strengths, and the results obtained are analogous to those in Figs. 3 and 4 and hence not repeated here.

In summary, we have extracted a presaddle dissipation strength of 5×10^{21} s^{-1} and exploited isospin effects on the evaporation residue spin distribution as a probe of presaddle dissipation effects in the framework of the dynamical Langevin model. We find that with increasing isospin of the system, the sensitivity of this spin distribution to nuclear dissipation decreases substantially. Furthermore, for ^{200}Os, this spin distribution is no longer sensitive to the nuclear dissipation. These results suggest that to accurately determine presaddle dissipation strength through the measurement of the evaporation residue spin distribution, it is best to yield those compound systems with low isospin.

This work is supported by National Natural Science Foundation of China under Grant No. 10405007.

[1] C. Schmitt *et al.*, Phys. Rev. Lett. **99**, 042701 (2007).
[2] J. Benlliure *et al.*, Phys. Rev. C **74**, 014609 (2006).
[3] V. Tishchenko *et al.*, Phys. Rev. Lett. **95**, 162701 (2005).
[4] B. Jurado *et al.*, Phys. Rev. Lett. **93**, 072501 (2004).
[5] U. Jahnke *et al.*, Phys. Rev. Lett. **83**, 4959 (1999).
[6] P. Fröbrich, Nucl. Phys. **A787**, 170c (2007).
[7] W. Ye, Phys. Lett. **B647**, 118 (2007).
[8] W. Ye, Phys. Rev. C **76**, 041601(R) (2007).
[9] D. Hilscher and H. Rossner, Ann. Phys. (Paris) **17**, 471 (1992).

[10] P. Paul and M. Thoennessen, Annu. Rev. Nucl. Part. Sci. **44**, 55 (1994).
[11] B. B. Back *et al*., Phys. Rev. C **60**, 044602 (1999).
[12] P. Fröbrich and I. I. Gontchar, Nucl. Phys. **A563**, 326 (1993).
[13] P. D. Shidling *et al*., Phys. Rev. C **74**, 064603 (2006).
[14] P. Fröbrich and I. I. Gontchar, Phys. Rep. **292**, 131 (1998).
[15] Y. Abe, S. Ayik, P. G. Reinhard, and E. Suraud, Phys. Rep. **275**, 49 (1996).
[16] W. Ye *et al*., Z. Phys. A **359**, 385 (1997).
[17] K. Pomorski *et al*., Nucl. Phys. **A679**, 25 (2000).
[18] P. N. Nadtochy, G. D. Adeev, and A. V. Karpov, Phys. Rev. C **65**, 064615 (2002).
[19] W. Ye, Prog. Theor. Phys. **109**, 933 (2003).
[20] I. I. Gontchar, L. A. Litnesvsky, and P. Fröbrich, Comput. Phys. Commun. **107**, 223 (1997).
[21] A. V. Ignatyuk *et al*., Sov. J. Nucl. Phys. **21**, 612 (1975).
[22] W. D. Myers and W. J. Swiatecki, Nucl. Phys. **81**, 1 (1966).
[23] W. D. Myers and W. J. Swiatecki, Ark. Fys. **36**, 343 (1967).
[24] M. Brack, J. Damgaard, A. S. Jensen, H. C. Pauli, V. M. Strutinsky, and C. Y. Wang, Rev. Mod. Phys. **44**, 320 (1972).
[25] G. Chaudhuri and S. Pal, Phys. Rev. C **65**, 054612 (2002).
[26] R. W. Hasse and W. D. Myers, *Geometrical Relationships of Macroscopic Nuclear Physics* (Springer-Verlag, Berlin, 1988).
[27] I. I. Gontchar, P. Fröbrich, and N. I. Pischasov, Phys. Rev. C **47**, 2228 (1993).
[28] M. Blann, Phys. Rev. C **21**, 1770 (1980).
[29] J. E. Lynn, *Theory of Neutron Resonance Reactions* (Clarendon, Oxford, 1969).
[30] P. Fröbrich, Phys. Rep. **116**, 337 (1984); Nucl. Phys. **A545**, 854 (1992).
[31] M. Thoennessen and J. R. Beene, Phys. Rev. C **45**, 873 (1992).
[32] A. Gavron *et al*., Phys. Rev. C **35**, 579 (1987).
[33] E. Strumberger *et al*., Nucl. Phys. **A529**, 522 (1991).
[34] N. D. Mavlitov, P. Fröbrich, and I. I. Gontchar, Z. Phys. A **342**, 195 (1992).
[35] G. R. Tillack *et al*., Phys. Lett. **B296**, 296 (1992).
[36] H. Singh *et al*., Phys. Rev. C **76**, 044610 (2007).
[37] G. van't Hof *et al*., Nucl. Phys. **A638**, 613 (1998).
[38] I. Diószegi *et al*., Phys. Rev. C **61**, 024613 (2000).
[39] I. Diószegi *et al*., Phys. Rev. C **63**, 014611 (2000).
[40] A. V. Karpov *et al*., Phys. Rev. C **63**, 054610 (2001).
[41] P. N. Nadtochy *et al*., Phys. Rev. C **72**, 054608 (2005).
[42] M. V. Borunov *et al*., Nucl. Phys. **A799**, 56 (2008).